US 20190137171A1

(19) **United States**

(12) **Patent Application Publication**

BARCLAY et al.

(10) **Pub. No.: US 2019/0137171 A1**

(43) **Pub. Date: May 9, 2019**

(54) **PRODUCTION OF LIQUID NATURAL GAS AND OTHER CRYOGENS USING A MULTI-STAGE ACTIVE MAGNETIC REGENERATIVE LIQUEFIER**

(71) Applicants: **Emerald Energy NW, LLC**, Bothell, WA (US); **Battelle Memorial Institute**, Richland, WA (US)

(72) Inventors: **John A. BARCLAY**, Bothell, WA (US); **Corey C. Archipley**, Lynnwood, WA (US); **Kerry Duane Meinhardt**, Richland, WA (US); **Edwin Charles Thomsen**, Pasco, WA (US); **Jamelyn Davis Holladay**, Kennewick, WA (US)

(21) Appl. No.: **16/031,939**

(22) Filed: **Jul. 10, 2018**

Related U.S. Application Data

(60) Provisional application No. 62/531,285, filed on Jul. 11, 2017.

Publication Classification

(51) **Int. Cl.**

F25J 1/02 (2006.01)

F25J 1/00 (2006.01)

(52) **U.S. Cl.**

CPC ***F25J 1/0227*** (2013.01); *F25J 2270/908* (2013.01); ***F25J 1/0022*** (2013.01)

(57) **ABSTRACT**

Apparatus and processes for liquefying process gases using multi-stage active magnetic regenerative refrigerators are disclosed. The apparatus and processes can be configured to liquefy process streams that liquefy below ~200 K, such as ethane, methane, argon, nitrogen, neon, hydrogen and/or helium process gases. Active magnetic regenerative liquefiers use multiple successive active magnetic regenerator stages, with each stage using a compositionally distinct magnetic refrigerant material having a distinct Curie temperature. In some aspects, the refrigerant material in each successive stage has a Curie temperature of about 20 K-40K different from that of neighboring stages. Heat transfer fluid flows are directed to improve system efficiency.

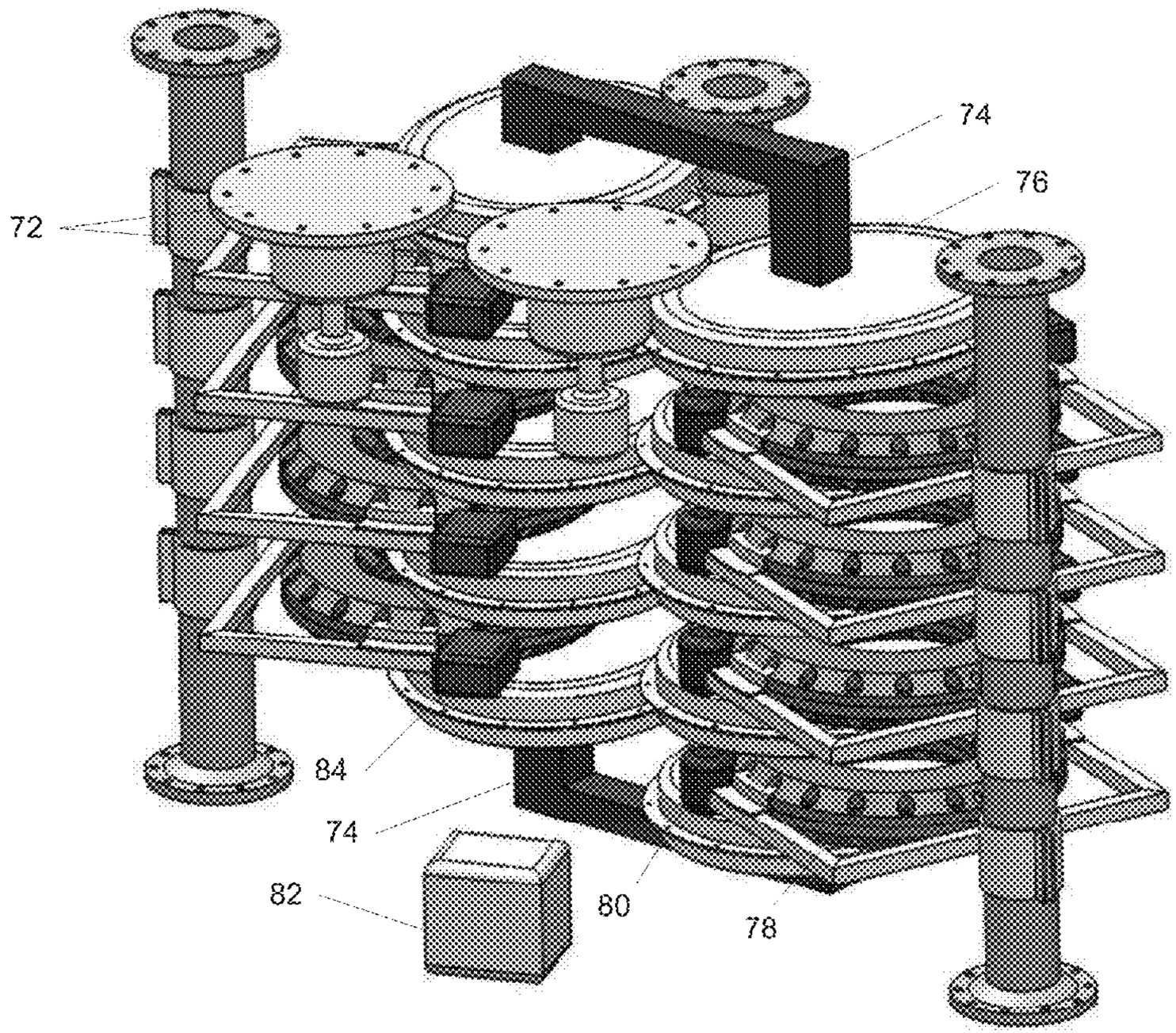

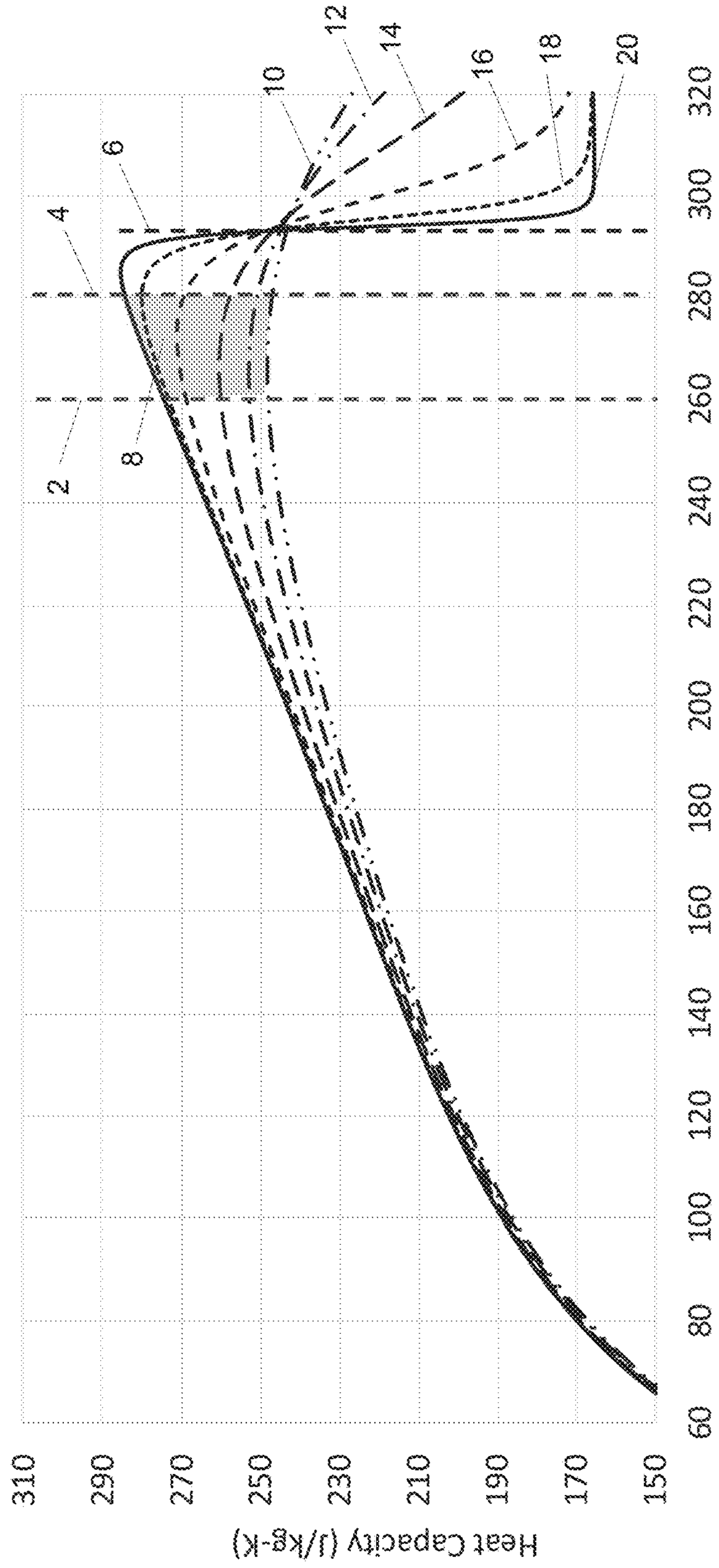
Heat Capacity (J/kg-K)
310
290
270
250
230
210
190
170
150
Temperature (K)
60
80
100
120
140
160
180
200
220
240
260
280
300
320
2
4
6
8
10
12
14
16
18
20

FIG. 1

FIG. 2

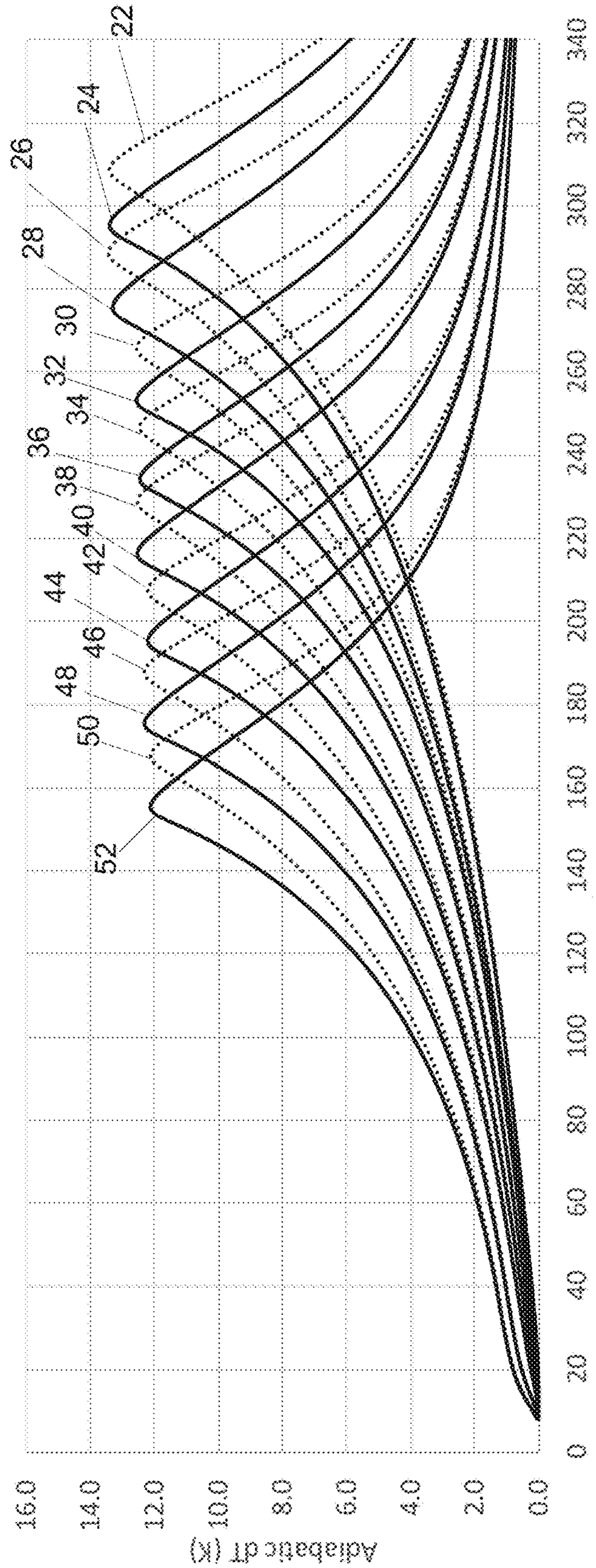
Adiabatic dT (K)
16.0
14.0
12.0
10.0
8.0
6.0
4.0
2.0
0.0
Temperature of Regenerator Material (K)
0
20
40
60
80
100
120
140
160
180
200
220
240
260
280
300
320
340
22
24
26
28
30
32
34
36
38
40
42
44
46
48
50
52

FIG. 3

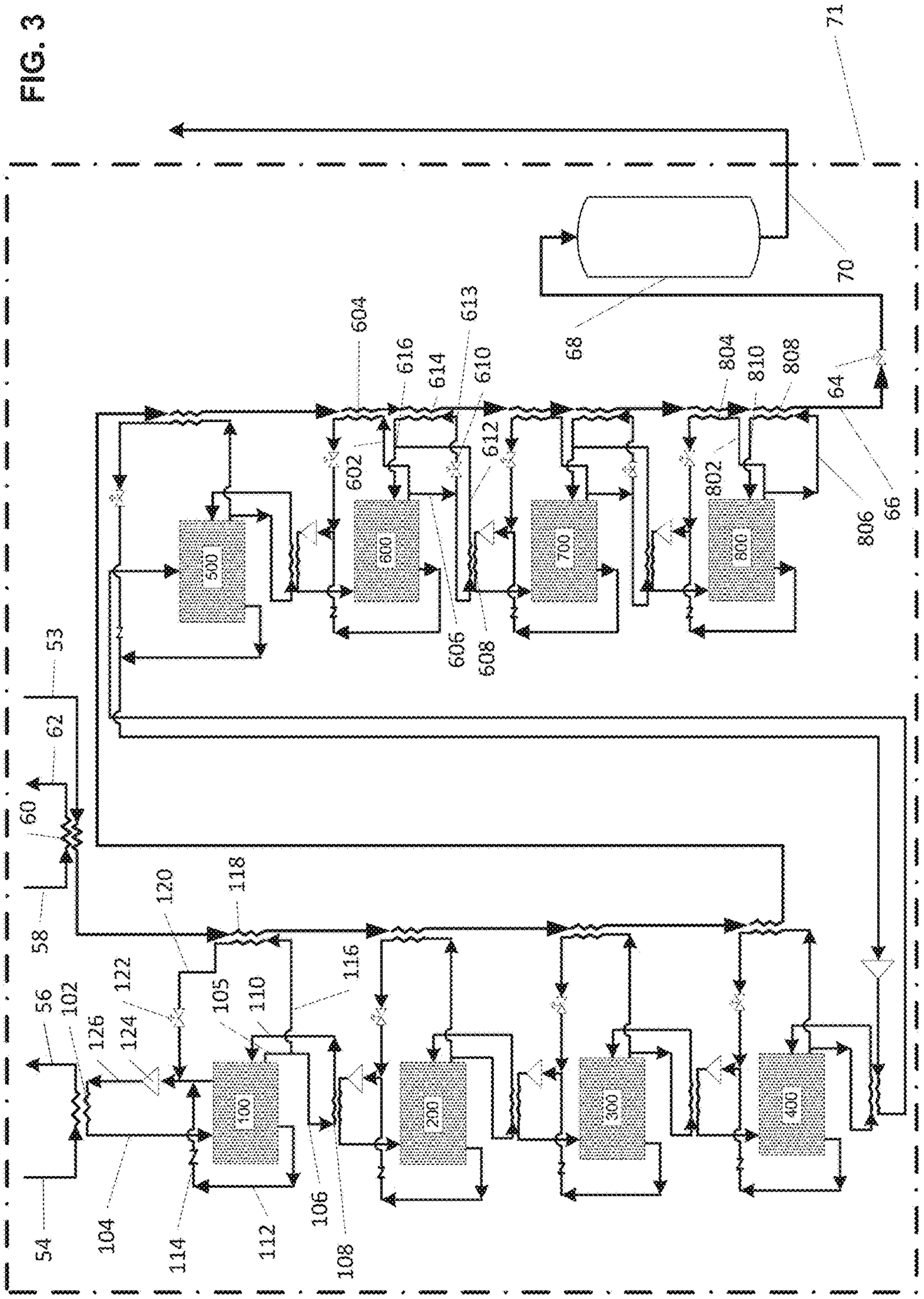
71
70
68
604
616
614
610
613
612
602
606
608
804
810
808
64
802
806
66
500
600
700
800
53
62
60
58
120
118
56
102
122
105
110
116
126
124
104
114
112
106
108
54
100
200
300
400

FIG. 4

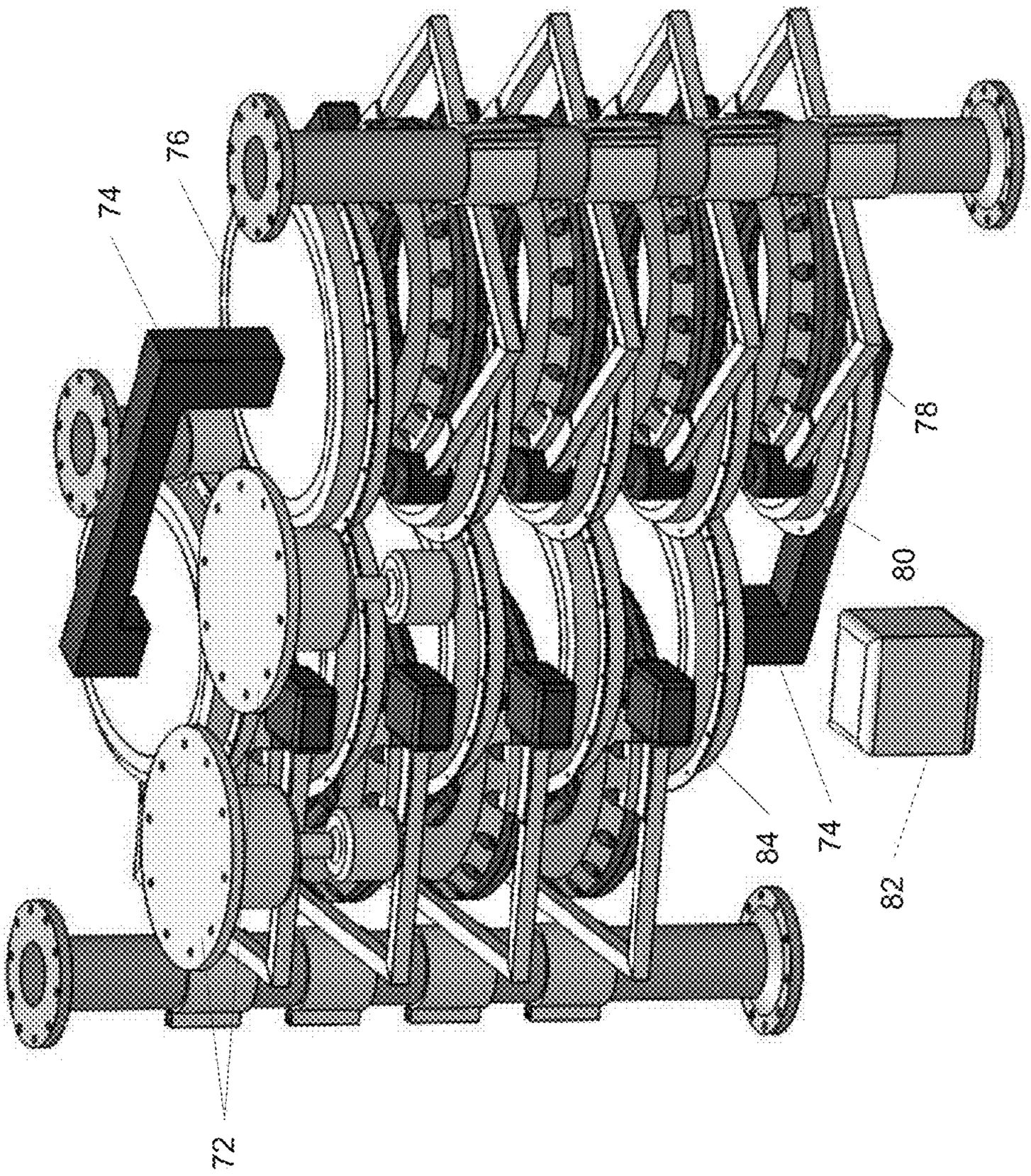

PRODUCTION OF LIQUID NATURAL GAS AND OTHER CRYOGENS USING A MULTI-STAGE ACTIVE MAGNETIC REGENERATIVE LIQUEFIER

CROSS REFERENCE TO RELATED APPLICATIONS

[0001] This application claims the benefit of U.S. Provisional Application No. 62/531,285, filed Jul. 11, 2017, which is herein incorporated by reference in its entirety.

ACKNOWLEDGMENT OF GOVERNMENT SUPPORT

[0002] This invention was made with government support under Contract No. DE-AC05-76RL0-1830 awarded by the U.S. Department of Energy. The government has certain rights in the invention.

FIELD OF THE DISCLOSURE

[0003] The present disclosure relates to magnetic refrigerators and, more particularly, to multi-stage active magnetic regenerative refrigerators configured as efficient liquefiers for cryogens such as liquid natural gas and liquid hydrogen.

BACKGROUND OF THE DISCLOSURE

[0004] In its various forms, energy is tightly linked to essentially all aspects of our life including food, water, environment, climate, quality of life, jobs, security, waste, and especially economics. In 2017 natural gas supplies >30% of US energy and is projected to supply almost 50% by 2050. Natural gas, a gas mixture of predominately methane, comes from many plentiful US sources such as shale play gas wells, associated gas from oil wells, coal bed gas, methane hydrates, biogas from anaerobic biomass waste digesters, and landfills. Numerous purification techniques are used to remove impurities to increase methane concentration to over 96% found in most pipeline-quality natural gas. Increased hydrogen gas adoption as fuel is projected to mimic natural gas use to reduce carbon intensity of energy use. The volumetric energy density of natural gas or hydrogen at low pressure can be increased by more than 600 times by cooling and liquefaction. As a result, liquid cryogens are excellent for storage, transport, and delivery of industrial gases and gaseous energy carriers such as liquid natural gas (LNG) and liquid hydrogen (LH_2). The energy efficiency of various types and sizes of liquefiers is characterized by their figure of merit (FOM) defined as the ratio of ideal to actual specific work required to liquefy a unit mass of any gas. The FOM depends upon gas composition, initial temperature and pressure of the gas, and final condition of the cryogenic liquid. When feedstock costs are modest, the actual input work is an important contribution to the cost of cryogens; thus, increasing liquefier FOM reduces cost of LNG, LH_2, and other cryogens.

[0005] Natural gas is primarily methane, so LNG provides a good example of available liquefier technology. The ideal specific work of liquefaction of methane is 1050 kJ/kg starting from ~290 K and one atmosphere. Three liquefaction techniques are used at most modern commercial large-scale LNG plants. These are: Cascade cycle designs with three different but usually pure gaseous refrigerants with three separate compressors; Mixed Refrigerant Cycle designs with refrigerant mixtures of 4-5 gases including choices among iso-pentane, butane, propane, ethane, methane, argon, and nitrogen with a single common compressor; and Turbo-Brayton cycle designs with pure nitrogen gas as refrigerant, a single compressor, and a cryogenic expander. These liquefiers have FOMs from 0.25 to 0.35 for large-scale, turn-key plants, and lower FOMs as capacity decreases below ~50,000 gpd of LNG in small-scale plants. The importance of higher FOMs motivated the on-going search for innovative liquefier technologies with higher FOMs, especially for small-scale units.

[0006] Because the magnetocaloric effect uses solid magnetic refrigerants rather than gases as refrigerants and magnetic field changes instead of gas compression to create a thermodynamic cycle, it was soon considered as an efficient refrigeration method above 4 K. The demonstration of a passive regenerative magnetic refrigerator near room temperature by Brown in 1976 and invention of the active magnetic regenerator (AMR) by Barclay and Steyert, Jr. U.S. Pat. No. 4,332,135A (1982) wherein magnetic solids are simultaneously active refrigerants and thermal regenerator media helped establish the possibility of higher FOMs with regenerative magnetic cycles from ~4 K up to ~290 K. Variations of AMR-based cryogenic refrigerator and cryogen liquefier designs developed since 1982 including reciprocating dual regenerators either fixed or moving solenoidal superconducting magnets, continuously rotating wheels with regenerator-rims using fixed Helmholtz pairs, partial Tokamaks, or other-shaped superconducting magnets, and fixed regenerators with nested rotating dipole magnets exist in the technical literature and USPTO patent data base. For example: see Lawton et al. U.S. Pat. No. 5,934,078 (1999), Pecharsky, et al. U.S. Pat. No. 5,887,449 (1999), Barclay, U.S. Pat. No. 4,408,463A (1983), DeGregoria et al. U.S. Pat. No. 5,249,424A (1993), and Barclay et al. U.S. Pat. No. 5,182,914A (1993). Numerous patents for different cryogenic magnetic refrigerants also exist such as Shashi et al. U.S. Pat. No. 4,849,017 (1989), Hashimoto U.S. Pat. No. 5,213,630 (1993), and Kuriyama et al. U.S. Pat. No. 5,447,034 (1995).

[0007] An AMR cycle has four steps: demagnetization of the AMR from high to low field with no heat transfer fluid flow; a hot-to-cold flow of heat transfer fluid at constant low field; magnetization of the AMR from low to high field with no fluid flow; and a cold-to-hot flow of heat transfer fluid at high field. After step 2 the cold heat transfer fluid absorbs heat from a thermal load before executing the cold to hot flow in step 4. The hot heat transfer fluid rejects heat to the heat sink after step 4 before it executes step 2. Unlike traditional techniques for liquefaction where work input is primarily from gas compression, work required for AMR cycles is primarily from overcoming unbalanced magnetic forces on magnetic regenerators during movement between low and high magnetic field regions. Adiabatic temperature changes are typically about 2 K per Tesla or a total of about 10-15 K for 5-6 T changes. Detailed numerical analyses predict AMRL designs can achieve FOMs of 0.5-0.7.

[0008] Many previously described active magnetic regenerative refrigerator (AMRR) prototypes with limited temperature spans have a single low-temperature stage coupled to a heat sink from gas-cycle refrigerators such as GM or pulse-tube devices or from cryogens such as LN_2 to achieve temperature spans of 4-20 K or 20-77 K. In some cases, two or more magnetic refrigerants are layered adjacent to one another in a single cylindrical AMR as shown for different

compositions of $Dy_xEr_{1-x}Al_2$ in U.S. Pat. No. 5,887,449 (1999) or for GdPd/GdNi in U.S. Pat. No. 5,249,424A (1993). To increase the FOM of AMRLs the hot temperature of the warmest AMRR stage must be near room temperature. For example, to increase the temperature span to 280 K to 120 K for LNG or from 280 K to 20 K for LH_2, as many as 4 to 13 different magnetic refrigerants with successively lower Curie temperatures may be used depending upon the cryogen being liquefied and optimum design for maximum FOM.

[0009] To best exploit use of multiple refrigerants, two distinct AMRR/AMRL design configurations have evolved: i) those with a multi-layer active magnetic regenerator with adjacent layers of magnetic refrigerants with sequentially colder Curie temperatures configured as a single-stage AMRL. For example, to produce LNG an AMRL operating from ~280 K to ~120 K could have from 4 to 8 layers in each regenerator, and ii) a multi-stage AMRL with each stage spanning 20 to 40 K using a single active magnetic regenerator fabricated with one magnetic refrigerant with sequentially colder Curie temperatures in each stage. For example, to produce LNG, an AMRL would have from 4 to 8 stages of AMRRs to span ~280 K and ~120 K. There are several design and operational differences between these two configurations such as the number and type of superconducting magnets required or need for controllable diversion flow valves in the multilayer designs.

[0010] U.S. Pat. No. 6,467,274 B2 by Barclay and Brook, (2002) describe an AMRL design with several AMRR stages operating from room temperature in parallel or series to cool and liquefy process streams of natural gas and hydrogen more efficiently. In this patent bypass flow is only used in parallel with the primary heat transfer fluid flow. In Cryogenics, 62, 185-192 (2014) T. Numazawa et al. review some experimental results and present conceptual analysis of several variations of multi-stage AMRL designs. These authors do not mention or use bypass flow but do suggest several different heat transfer fluids for various stages.

[0011] Neither the technical literature nor the patent literature disclose several of the features of multi-stage AMRLs disclosed that leverage FOM enhancing effects of bypass flow that reduces approach temperatures in counterflow heat exchangers while simultaneously reducing entropy generation by properly balancing heat transfer fluid flows in the magnetized and demagnetized steps of the AMR cycle plus satisfying constraints of the 2^{nd} law of thermodynamics on adiabatic temperature changes in AMRs with irreversible entropy mechanisms, selecting magnetocaloric alloy refrigerants with peak efficiencies for multiple specific temperature ranges for each stage of operation to liquefy natural gas or other cryogens disclosed herein.

SUMMARY OF THE DISCLOSURE

[0012] Disclosed herein is a process for liquefying natural gas or other process gases comprising the following steps, with or without additional steps:

[0013] introducing a high-pressure helium or liquid propane heat transfer fluid into each stage of a multi-stage active magnetic regenerative refrigerator apparatus wherein each stage comprises (i) a high magnetic field section in which the heat transfer fluid flows from a cold side to a hot side through at least one magnetized regenerator of at least one magnetic refrigerant, (ii) a first no heat transfer fluid flow section in which the regenerator is demagnetized, (iii) a low magnetic field or demagnetized section in which the heat transfer fluid flows from a hot side to a cold side through the demagnetized regenerator, and (iv) a second no heat transfer fluid flow section in which the regenerator is magnetized;

[0014] continuously introducing within each stage a separate flow of the heat transfer fluid from the cold side of the low magnetic field or demagnetized section into the cold side of the high magnetic field or magnetized section; and

[0015] continuously separating a portion of the cold heat transfer fluid flowing from the cold side of the low magnetic field or demagnetized section of each stage to create an unbalance flow stream from each stage returned through a process gas heat exchanger at each stage to cool the process gas before the heat transfer fluid stream rejoins the primary heat transfer stream near the hot temperature of each stage near the inlet to the fluid circulating means.

[0016] Disclosed herein in one embodiment is a process for liquefying a process gas comprising at least one of the following steps, with or without additional steps:

[0017] introducing heat transfer fluid into an active magnetic regenerative refrigerator apparatus that comprises from about 4 to about 13 successive stages, wherein each stage comprises an independently compositionally distinct magnetic refrigerant material having an independent Curie temperature, and wherein the first stage has the highest Curie temperature and the last stage has the lowest Curie temperature;

[0018] flowing different rates of heat transfer fluid through each stage of the active magnetic regenerative refrigerator apparatus which enables a multistage liquefier to be easily cooled-down during start up from 280 K gradually stage by stage from 280 K until all magnetic refrigerants are cooled below their respective Curie temperatures and into their optimum operating temperature range, i.e. 280-260 K for first stage, 260-240 K for the second stage, 240-220 K, and so on down to the bottom stage at 140-120 K;

[0019] flowing bypass flow from each stage through a process heat exchanger to remove all sensible heat from a process stream to cool it by the same temperature as the stage operates over; and

[0020] flowing primary heat transfer fluid through a thermal load heat exchanger to absorb reject heat from the next lower stage and in stages where the process stream liquefies, to absorb the latent heat of liquefaction plus any parasitic heat leaks into the stage where liquefaction occurs.

[0021] Further disclosed herein is an apparatus comprising at least one of the following features:

[0022] an active magnetic regenerative liquefier module comprising multiple successive stages, wherein each stage comprises an independently compositionally distinct magnetic refrigerant material having Curie temperatures preferably 20-30 K apart between successively adjacent stages although ~40 K differences in Curie temperatures may be used if fewer stages are used to span the same temperature, e.g., ~280 K to ~120 K for LNG, and the stages are arranged in successive Curie temperature order and magnetic refrigerant material mass order with a first stage having the highest Curie temperature and highest magnetic refrigerant material mass and the last stage having the lowest Curie temperature and lowest magnetic refrigerant material mass;

[0023] constraint of each magnetic refrigerant to operate near and below its Curie temperature throughout an entire active magnetic regeneration cycle of each stage;

[0024] temperature spans ranging from 20-30 K per stage resulting in multiple stages to cool from 280 K to 120 K;

[0025] porous magnetocaloric regenerator materials for maximized adiabatic temperature changes and field and large temperature-dependent thermal mass differences from heat capacity for specific and narrow operating temperature ranges below their respective Curie temperatures; and

[0026] magnetic materials with maximum adiabatic temperature changes at average hot and cold temperature of each stage such that the ΔT's best satisfy the 2^{nd} law of thermodynamics illustrated by the equation $T_{HOT}/T_{COLD}=\Delta T_{HOT}(1+\delta)/\Delta T_{COLD}$ where δ depends upon the amounts of inevitable internal regenerator irreversible entropy creation during an AMR cycle.

[0027] Additional advantages and features of the apparatus and methods disclosed herein will be set forth in part in the description which follows, and in part will become apparent to those skilled in the art upon examination of the following or may be learned by practice of the disclosure. The foregoing will become more apparent from the following detailed description, which proceeds with reference to the accompanying figures.

BRIEF DESCRIPTION OF THE DRAWINGS

[0028] The foregoing will become more apparent from the following detailed description, which proceeds with reference to the accompanying figures, in which like reference numerals designate like elements and wherein:

[0029] FIG. **1** is a graph showing temperature and field dependent heat capacity of ferromagnetic refrigerants.

[0030] FIG. **2** is a graph showing adiabatic temperature changes for low to high (up) and high to low (down) field of eight ferromagnetic refrigerants used for a 280 K to 120 K AMRL.

[0031] FIG. **3** is a partially schematic diagram of an active magnetic regenerative liquefier that includes more than one single-stage active magnetic regenerative refrigerator (AMRR) coupled together in series from cold to hot operating temperatures.

[0032] FIG. **4** is a partially schematic diagram of an eight stage AMRL using rotary wheel configuration of the magnetic regenerators in each stage with a set of ten slightly elliptically shaped superconducting magnets in a magnetic circuit to efficiently create the high field regions for all eight stages with primary components labelled.

[0033] It will be understood that the appended drawings are not necessarily to scale, and that they present simplified, schematic views of many aspects of systems and components of the present invention. Specific design features, including dimensions, orientations, locations and configurations of various illustrated components may be modified, for example, for use in various intended applications and environments. It will also be appreciated that various features from one drawing may be omitted in alternative embodiments, and that various illustrated features may be used in combination with features from other drawings to provide additional embodiments, and that such combinations, whether resulting from omission or combination, are intended to be within the scope of the disclosure herein.

DETAILED DESCRIPTION OF THE DISCLOSURE

[0034] Disclosed herein are processes and systems for efficient multistage active magnetic regenerative refrigerators configured for liquefying any process stream that liquefies below ~200 K including ethane, methane, argon, nitrogen, neon, hydrogen, or helium process gases. In this disclosure we have identified specifications for multistage AMRL designs that can achieve FOM of 0.6-0.7 that none of the existing conventional liquefiers can achieve.

[0035] Proper selection of magnetic refrigerants is key to successful liquefiers that are both cost effective and highly efficient. Good magnetic refrigerants have large magnetic moments to provide maximum entropy change from changes in magnetic field. The accompanying magnetocaloric effect of a good material is confined to a finite temperature range around its ferromagnetic ordering temperature where the magnetic entropy is strongly temperature and field dependent. To take maximum advantage of bypass flow it is important to maximize the difference between the high-field and low-field thermal mass of magnetic refrigerants. The thermomagnetic properties of the refrigerants must simultaneously satisfy numerous other criteria such as: i) satisfying the adiabatic temperature changes as a function of temperature to satisfy the 2nd law of thermodynamics and ii) allowance for inevitable creation of some irreversible entropy even in the best optimized regenerator designs.

[0036] The magnetic refrigerants in the AMR beds have a difference in thermal mass which is the product of heat capacity per unit mass times the mass of magnetic refrigerant (or just heat capacity in this case because the mass of magnetic material in a magnetic regenerator doesn't depend upon temperature or magnetic field). The heat capacity of a ferromagnetic material below the Curie temperature (ordering temperature) is smaller in higher magnetic fields than at lower or zero magnetic fields. However, this difference switches at the Curie temperature because the heat capacity in higher magnetic fields decreases slowly as the temperature increases while the heat capacity in low or zero fields drops sharply at the Curie temperature such that the heat capacity at higher fields becomes larger than the heat capacity in lower or zero magnetic fields. This means the difference in thermal mass between a magnetized AMR bed and a demagnetized AMR bed changes sign at the Curie temperature and the net difference in thermal mass for an AMR cycle spanning across the Curie temperature rapidly decreases with increasing temperature. Therefore, the optimal amount of bypass flow for an AMR cycle that extends above the Curie temperature will rapidly decrease to zero. Simultaneously an AMR cycle operated this way will become less efficient due to increased intrinsic entropy generation in such an AMR cycle and due to insufficient bypass flow to pre-cool the same amount of hydrogen process gas.

[0037] In the design of the novel processes and systems, the importance of selecting and controlling the hot sink temperature and temperature span to maximize the difference in thermal mass (and thereby the amounts of bypass flow) is recognized. First, the dynamic T_{HOT} is always ΔT_{HOT} less than the Curie temperature of the magnetic refrigerant at the hot end of the regenerator (i.e., the outermost refrigerant in the layered rim of the wheel in FIG. **1**) at its maximum during the magnetization step of the AMR cycle. T_{HOT} is the environmental temperature where the heat is dumped. The dynamic T_{HOT} is the increase in temperature caused by inserting the regenerator into the magnetic field. The maximum dynamic T_{HOT} depends on where it is in the cycle, but generally the maximum is $T_{HOT}+\Delta T_{HOT}$. This can

be done by setting a fixed heat sink temperature to anchor T_H which in turn yields the largest difference in thermal mass between high and low magnetic fields.

[0038] The second aspect of the difference in thermal mass in high and low magnetic fields is that it decreases steadily as the cold temperatures in the regenerator decrease below the Curie temperature (s) of the magnetic refrigerants. Hence, the magnetic materials in an AMR bed must operate in temperature spans when magnetized of T_H $\Delta T_{HOT} \leq T_{Curie}$ and $T_C+\Delta T_{COLD}$ equal to ~20 K$<T_{Curie}$ and when demagnetized, between $T_H-\Delta T_{HOT}$ and $T_C-\Delta T_{COLD}$ which are 20 K apart. T_C represents cold temperatures of a slice of magnetic regenerator at any point in the AMR as it executes its tiny magnetic Brayton cycle. ΔT_{COLD} represents the temperature drop caused by the magnetocaloric effect when the regenerator is removed from the magnetic field. If larger temperature spans with optimum differences in thermal mass are desired (as required for very high FOM), layers of magnetic materials with descending Curie temperatures must be used in the AMR bed.

[0039] Gadolinium is an excellent magnetic refrigerant and has been generally accepted as the reference material against which other refrigerants are compared. It has a simple ferromagnetic ordering temperature of ~293 K and exhibits an adiabatic temperature change of ~2 K/Tesla over practical magnetic field strengths (up to ~8 T). It also has a large difference in field-dependent thermal mass just below its Curie temperature. Introduction of alloying additions of another lanthanide metal reduces the magnetic-ordering temperature of Gd without much effect on the total magnetic moment per unit volume and the change in magnetization with temperature near a sharp ordering temperature. Homogeneous alloys of Gd with other rare earth metals (Nd, Tb, Er, Dy, Ho) or Y make superior magnetic refrigerants as well. Other potential rare earth elemental refrigerants such as Ho and Er have more complex magnetic ordering phenomenon but when alloyed with Gd these effects tend to be reduced at high magnetic fields.

[0040] FIG. **1** shows the measured heat capacity of ferromagnetic Gd metal as a function of temperature for several applied magnetic fields. The Curie temperature **6** is at 293 K and the total heat capacity which is the sum of electronic, lattice, and magnetic contributions are shown at 0.05 T **20**, 0.35 T **18**, 1.0 T **16**, 3.0 T **14**, 6.0 T **12**, and 9.0 T **10**. These curves show that below the Curie temperature, the heat capacity in low applied field is larger than that at higher fields, i.e. ~10% larger between 0.05 T and 6 T for about 30 K below the Curie temperature. The thermal mass is the integral of heat capacity over a temperature span; the difference in thermal mass **8** of Gd between 260 K **2** and 280 K **4**, is large enough to require a ~8% larger heat transfer fluid flow to cool Gd from 280 K to 260 K at low field than at high field. This is a unique effect that doesn't occur in gas cycle liquefiers.

[0041] In properly designed AMRLs using ferromagnetic refrigerants just below their Curie temperatures, this effect enables unbalanced or bypass flow of cold heat transfer fluid that can be used to completely cool process stream from the hot to the cold temperature in each stage of a multistage AMRL. This enables three performance enhancing effects; the first is to increase the FOM by about 30%; second, it balances the different heat transfer fluid flows required in the magnetized, and demagnetized regenerators; and third, it reduces the mass of magnetic refrigerant required for a given cooling power by several times. Each stage of the disclosed AMRL has separate heat transfer fluid flow circuits so can independently optimize the amount of bypass flow required to optimally increase FOM from the temperature approach in the process heat exchangers and from imbalanced flows in the two field regions of the AMR cycle.

[0042] Proper selection of ferromagnetic refrigerants for use over optimum specific temperature spans for maximum bypass impact is an important feature of this multistage AMRL.

[0043] FIG. **2** shows adiabatic temperature changes (up and down) for 8 specific magnetocaloric rare earth alloys used in the 8 stage AMRL. The adiabatic temperature changes upward (dT UP) represented by the solid lines are caused by the magnetic field being applied from the temperature on the x axis. The adiabatic temperature changes downward (dT DOWN) represented by the dashed lines are caused by the magnetic field being reduced (or ideally removed entirely to get the greatest effect in temperature) from the starting temperature on the x-axis. Below 260 K magnetocaloric alloys other than Gd have been identified that provide a magnetocaloric effect with a similar magnitude to Gd when it is in its desired operating range 260-280 K. Alloys of Gadolinium including Gadolinium-Terbium (Gd_xTb_x), Gadolinium-Erbium (Gd_xEr_x), Gadolinium-Dysprosium (Gd_xDy_x), Gadolinium-Holmium (Gd_xHo_x), Gadolinium-Neodymium (Gd_xNd_x), Gadolinium-Cerium (Gd_xCe_x) and combinations hereof are specific alloys claimed as magnetic refrigerants within this embodiment. Specific alloy compositions have been determined to create the desired magnetocaloric effect in terms of magnitude for various temperature ranges beginning with common feed stock temperatures for natural gas (~280-290 K) down to natural gas' liquefaction temperature at atmospheric pressure (111 K). Items **22** and **24** represent dT DOWN and dT UP for Gadolinium respectively. The peak in curve **24** is at the Curie temperature for Gd of ~293 K. Items **26** and **28** represent dT DOWN and dT UP for $Gd_{0.83}Dy_{0.17}$ respectively. The peak in curve **28** is at the Curie temperature for $Gd_{0.83}Dy_{0.17}$ of ~273 K. Items **30** and **32** represent dT DOWN and dT UP for $Gd_{0.30}Tb_{0.70}$ respectively. The peak in curve **32** is at the Curie temperature for $Gd_{0.30}Tb_{0.70}$ of ~253 K. Items **34** and **36** represent dT DOWN and dT UP for $Gd_{0.69}Er_{0.31}$ respectively. The peak in curve **36** is at the Curie temperature for $Gd_{0.69}Er_{0.31}$ of ~232 K. Items **38** and **40** represent dT DOWN and dT UP for $Gd_{0.32}Dy_{0.68}$ respectively. The peak in curve **40** is at the Curie temperature for $Gd_{0.32}Dy_{0.68}$ of ~213 K.

[0044] Items **42** and **44** represent dT DOWN and dT UP for $Gd_{0.15}Dy_{0.85}$ respectively. The peak in curve **44** is at the Curie temperature for $Gd_{0.15}Dy_{0.85}$ of 193 K. Items **46** and **48** represent dT DOWN and dT UP for $Gd_{0.27}Ho_{0.73}$ respectively. The peak in curve **48** is at the Curie temperature for $Gd_{0.27}Ho_{0.73}$ of 173 K. Items **50** and **52** represent dT DOWN and dT UP for $Gd_{0.16}Ho_{0.84}$ respectively. The peak in curve **52** is at the Curie temperature for $Gd_{0.16}Ho_{0.84}$ of 153 K. Notable in the graph is the consistent peak values of dT UP, dT DOWN, and the ~20 K different in Curie temperatures for each layer. The regularity in adiabatic temperature changes in succinct temperature ranges allows for a staged device to work very well. This is really important for cool-down of any magnetic refrigerator; it is much easier to do with the herein disclosed multistage AMRL than other designs.

[0045] In active magnetic regenerative liquefier (AMRL) designs rejection and absorption of heat are achieved by the temperature increase or decrease of magnetic refrigerants in regenerators upon isentropic magnetization or demagnetization combined with reciprocating flow of heat transfer gas. The cycle steps that magnetic refrigerants in an active magnetic regenerator (AMR) execute are: i) magnetization with no heat transfer gas flow; ii) cold-to-hot heat transfer gas flow at constant magnetic high field; iii) demagnetization with no heat transfer gas flow; and iv) hot-to-cold heat transfer flow at constant low or zero field. The AMR cycle of one or more refrigerants thermally connected by heat transfer fluid flow (e.g., a gas) in AMRR stages can be used to design excellent liquefiers whose potential for high performance comes from:

[0046] Almost reversible nature of magnetization-demagnetization steps in an AMR cycle at up to hertz frequencies for certain magnetic refrigerants. In contrast, it is inherently difficult to reversibly achieve high compression ratios, high throughput, and high efficiency in gas compression because of fundamentally poor thermal conductivity of low-density gases such as hydrogen or helium;

[0047] Efficient internal heat transfer between porous working refrigerant solids and flowing heat transfer fluids (e.g., a gas) in AMR cycles can maintain small temperature differences at all times during the cycle by using geometries with high specific areas such as ~10,000 m^2/m^3 in high-performance regenerators;

Efficient cooling of the natural gas or other process gases and the AMRR heat transfer gas. This is a critical element of efficient cryogenic liquefier design. The huge impact on FOM of this single design feature illustrates the importance of reduction of approach temperatures in process heat exchangers in cryogenic liquefiers. Conventional gas cycle liquefiers with only two to four heat exchanger stages inherently limit their FOM to less than 0.50 before other real component inefficiencies are incorporated. Reducing the approach temperatures in process heat exchangers by using counterflowing bypass flow of a small percentage of heat transfer gas is a unique feature of AMRL designs to achieve a FOM greater than 0.5.

[0048] The above-explained desired features can be achieved by incorporating into the systems and processes at least one, and preferably a combination, of the following inventive aspects disclosed herein:

[0049] Continuous bypass flow to continuously pre-cool the process gas stream. The bypass gas flow is determined by the amount necessary to completely pre-cool the process gas stream while maintaining small 1-2 K temperature approaches between counter-flowing bypass gas and process gas;

[0050] The heat capacity of the magnetic refrigerant changes with the magnetic field, especially in the temperature region from the Curie temperature to ~25-30 K lower. Therefore, the thermal mass, or heat capacity multiplied by the refrigerant mass, will also vary. To take advantage of this phenomena unique to ferromagnetic refrigerants in an AMR cycle, the mass flow rate of heat transfer gas in the hot to cold flow region (low field) of the AMR cycle must be several percent (e.g., 2-12%, more particularly 2%, 3%, 4%, or 5%) larger than the mass flow rate of heat transfer gas in the cold to hot flow region (high field) of the same AMR cycle to balance (i.e., equivalent or close to the same) the energy transfers in the low and high field regions of the AMRR executing an efficient AMR cycle; the difference in heat transfer gas flows is separated from the heat transfer flow after the hot to cold flow in the AMRR to create a cold bypass stream of heat transfer gas that is warmed as it is returned to the hot temperature of the AMRR by flowing through the process stream heat exchangers in the AMRR;

[0051] The temperature difference between the bypass heat transfer entering the process heat exchanger at a first cold inlet temperature and the process gas exiting the process heat exchanger at a first cold exit temperature is 1 to 5 K, more particularly 1 to 2 K;

[0052] The magnetic refrigerant operates at or below its Curie temperature throughout an entire AMR cycle because this is the temperature span where the difference of thermal mass between magnetized and demagnetized magnetic refrigerants is maximized;

[0053] The sensible heat of the process gas is entirely removed by the bypass flow heat exchanger and/or

[0054] The increased process heat thermal load from latent heat of the liquefaction of the process gas can be accommodated in a staged AMRL by increasing the size of the liquefying stage (and all series-connected stages above it) to match the design conditions of the process stream. This is much more difficult to do in other types of liquefiers than in the multi-stage AMRL.

[0055] To achieve high FOM, eight stages, each with a different ferromagnetic refrigerant with large magnetocaloric effect near their Curie temperatures, are connected in series as illustrated in FIG. **3**. In this embodiment each single regenerator rotary stage **100** has continuous cold bypass heat transfer gas flow **116**, **602**, **802** through eight process heat exchangers to give very small temperature approaches between natural gas and bypass heat transfer gas. The temperatures, energy and mass flows in this 280 K to 120 K AMRL with a 6 T field change in a 1-Hz cycle while producing 1000 gpd of LNG were calculated and shown below. The input work rates, thermal-load and heat-rejection energy flows, mass of refrigerant per stage, and FOM were obtained.

[0056] The exhaust heat of the AMRL from the 1^{st} stage **100** of the 8-stage configuration in FIG. **3** is rejected into a hot heat sink exchanger **102** by the heat transfer gas **126** in the cold to hot flow. The hot heat sink exchanger is cooled by a fluid flow **54**, **56** such as water-glycol mixture from the controllable hot heat sinker chiller. This chiller stream **58**, **62** also cools **60** the process stream gas **53** to ~280 K before it enters the process stream heat exchangers **118**.

[0057] The bypass heat transfer fluid **120** exiting the bypass heat exchanger is combined with a hot heat transfer fluid flow **112** exiting the high magnetic field section (i.e., layer **1***b*). In certain embodiments, the bypass heat transfer fluid exiting the bypass heat exchanger is combined with the hot heat transfer fluid flow at the suction side of a pump **124** that circulates the heat transfer gas. The combined bypass heat exchanger exit fluid flow and hot heat transfer flow is introduced into the highest Curie temperature stage via introduction conduit **104**. The hot heat transfer flow is fluidly coupled to the bypass heat exchanger exit fluid flow via conduit **116**. In certain embodiments, the mixed bypass heat exchanger exit fluid flow and hot heat transfer flow may pass through an optional chiller hot heat sink exchanger **102**.

The exhaust heat from a thermodynamic cycle such as the AMRR must be removed to complete the cycle and the temperature-controlled chiller is the means to do this. It also allows setting of the steady-state T_{HOT} of the AMRL at 280 K.

[0058] In the rotary wheel configuration, the wheel rotation continually causes regenerator segments in the rim of the wheel to be entering the high field region simultaneously as other identical layered regenerator segments are entering the low field region of the wheel.

[0059] Each rotary stage of AMRL apparatus of FIG. **3** includes an annular regenerator of one porous magnetic refrigerant material. The rotary AMRR apparatus is divided into four sections (listed in order of wheel rotation): (i) a high magnetic field section in which the heat transfer gas flows from a cold side to a hot side through the magnetized bed(s), (ii) a first no heat transfer gas flow section in which the bed(s) are demagnetized, (iii) a low magnetic or demagnetized field section in which the heat transfer gas flows from a hot side to a cold side through the demagnetized bed(s), and (iv) a second no heat transfer gas flow section in which the bed(s) are magnetized. Circumferential seals are provided in the no circumferential heat transfer gas flow sections to prevent the heat transfer gas flow. Radial or axial seals are provided in the radial or axial heat transfer gas flow sections to prevent the heat transfer gas flow over, under, or around regenerators so only flow through the regenerator occurs. Each multistage magnetic regenerator magnetic regenerator is divided into compartments wherein the compartments eliminates circumferential flow of heat transfer gas through the porous regenerators while allowing radial flow of heat transfer gas.

[0060] The heat transfer fluid exits the CHEX and into a T-junction in which a portion of the heat transfer fluid bypasses the high magnetic field section and instead is directed to an inlet of a bypass gas heat exchanger **118**. The flow at the T-junction may be controlled a bypass flow control valve **122**. In certain embodiments, 3-12%, particularly less than 12%, more particularly less than 8%, and most particularly 6%, of the heat transfer fluid is diverted to the bypass gas heat exchanger. The remaining heat transfer fluid **110** is introduced as the cold flow into the rotating regenerator at the high magnetic field section.

[0061] The cold HTF flows in a radial direction through the high magnetized bed, heating the HTF. The hot HTF exits the high magnetic field section via an HTF outlet duct. The hot HTF exits the high magnetic field section and is introduced via a conduit to into a hot heat exchanger (HHEX) **102**. The HHEX cools the heat transfer fluid down to a suitable temperature for introduction as the hot flow **104** into the low magnetic or demagnetized field section

[0062] As mentioned above, the bypass HTF is introduced into a bypass HEX **118**. The bypass HTF **116** cools the process gas **53** that is also introduced into the bypass HEX **118**. The bypass HTF exiting the bypass HEX **118** is mixed with the hot HTF flow exiting the high magnetic field section. The mixed bypass HEX and hot HTT flow **126** is introduced into the HHEX **102**.

[0063] For optimal heat transfer, different mass flow rates of heat transfer gas are required in these two stages (i.e., magnetized vs. demagnetized), and this is accomplished by bypass of some cold heat transfer gas from the hot-to-cold flow step before the cold-to-hot flow step of the cycle. For example, maximum use of continuous flow of cold sensible heat in the bypass stream as it returns to higher temperatures in a counterflow heat exchanger to continuously cool a process gas stream can increase the FOM of an AMRL from ~0.35 in conventional gas-cycle liquefiers to ~0.60 or more in AMRLs. Besides increasing the FOM, the use of bypass stream to continuously and completely cool the process gas significantly reduces the refrigeration cooling capacity per AMRR stage and thereby reduces the mass of magnetic refrigerants required in the AMRL. Rotary AMRLs intrinsically have continuous bypass gas flow for continuous pre-cooling of a process gas stream while reciprocating AMRLs need at least two sets of dual regenerators with proper phasing in/out of the magnetic field with three-way valves to provide continuous bypass gas flow into the process heat exchangers.

[0064] The series of stages work in tandem to cool a natural gas or natural gas process stream in the following fashion (FIG. **3**). The coldest stage **800** running a 4-stage AMR cycle cools the process stream from 140 K to 120 K by using a main counter-flow heat exchanger **808** and a bypass counter-flow heat exchanger **804**. The total load shared by each heat exchanger is the cooling power required to provide the 20 K span of the process stream mass flow. The fractional split of the total load between the two heat exchangers is determined by the natural gas mass flow and the dT DOWN and UP for this stage's refrigerant. The rejected heat from this stage includes the process stream load, the work rate, irreversible losses, and any parasitic leaks. This rejected heat becomes the main load for the next stage up.

[0065] The next stage **700** has two loads to cool. One is the process stream **53**, cooling it from 160 K-140 K. The other is the rejected heat from the coldest stage as discussed above. Like the stage above, these loads will be shared by both the main heat exchanger and the bypass heat exchanger. In some cases, the main heat exchanger may cool both the rejected heat from the coldest stage and a portion of the process stream load. The rejected heat from this stage includes the process stream cooling load, the rejected heat from the previous stage, the work rate, irreversible losses, and any parasitic leaks.

[0066] The next stages follow this pattern of cooling the rejected heat from the colder stages while also cooling the process stream in 20 K spans using the main heat exchanger, bypass, or both. These stages are rejecting heat to the warmer stages until the warmest stage can reject the heat to the atmosphere or a basic chiller (~285 K). The calculation below describes in detail how the loads on each stage must grow to cool the rejected heat from the cold stages below as the process stream is cooled over a broader temperature range, as well as the total work, parasitic loads, and irreversible losses add up from stage to stage.

[0067] Depending on the number of stages and exact temperature spans per stage, there is a stage or set of stages where natural gas liquefaction occurs. In this case, the latent heat associated with this phase change places a significant load on the stages handling the liquefaction. Regenerator size, refrigerant type, and splitting of the process stream load with the rejected heat below will accommodate this nonlinear impact to the needed cooling power. In FIG. **3**, the sixth stage **600** is where liquefaction occurs. At this stage the primary HTF leaving the device **600** at the cold end is split into three streams. A stream **606** picks up the heat rejected from the colder stage **700**. Another stream **613** picks up a

load from the process stream from cold heat exchanger **614**. A majority of the liquefaction occurs in CHEX **614**, where the process stream is cooled from its dew point to its bubble point. A valve **610** is placed in this line to manage the flow. The third stream, the bypass stream **602**, picks up load from the process stream in a CHEX **604** and cools the process stream to its dew point. Stages warmer than the stages that manage the liquefaction are sized and tuned to manage the substantial amounts of rejected heat from the liquefying stages while also proving the cooling power for the ~20 K span of process stream cooling. Stages colder than the liquefying will provide the cooling power to sub-cool a now liquid process stream while picking up the rejected heat from the colder stage below.

[0068] The liquefied cryogen ultimately leaves the coldest stage **800** is stored in an insulated vessel **68** inside the cold box **71** (which houses all the AMR stages and magnets). The liquid cryogen is dispensed outside of the cold box **71** through an insulated hose **70**.

[0069] Performance and design specs for an 8-stage, single-refrigerant per stage AMRL configured in series to liquefy 300 psia natural gas feedstock. Enthalpies for natural gas are used every 20 K from 280 K Thot to 120 K Tcold temperatures to determine design specs per regenerator and resultant FOM as a 1000 gpd liquefier. A small process heat exchanger pressure drop allowance is taken as 0.5 psia.

Values of the enthalpy (h), density (φ, and entropy(s) for methane (CH_4) at 300 psia and 280 K were calculated using the property code named Refprops and are given as:

$$h_{CH41} := 847.88 \cdot \frac{\text{kJ}}{\text{kg}}$$

$$\rho_{CH4280} := 14.918 \cdot \frac{\text{kg}}{\text{m}^3}$$

$$s_{CH4280} := 4.9161 \cdot \frac{\text{kJ}}{\text{kg} \cdot \text{K}}$$

Methane enthalpy at 299.5 psia and 260 K was calculated using Refprops and is given as:

$$h_{CH42} := 801.08 \cdot \frac{\text{kJ}}{\text{kg}}$$

Methane enthalpy at 299.0 psia and 240 K was calculated using Refprops and is given as:

$$h_{CH43} := 753.96 \cdot \frac{\text{kJ}}{\text{kg}}$$

Methane enthalpy at 298.5 psia and 220 K was calculated using Refprops and is given as:

$$h_{CH44} := 705.83 \cdot \frac{\text{kJ}}{\text{kg}}$$

Methane enthalpy at 298.0 psia and 200 K was calculated using Refprops and is given as:

$$h_{CH45} := 655.46 \cdot \frac{\text{kJ}}{\text{kg}}$$

Methane enthalpy at 297.5 psia and 180 K was calculated using Refprops and is given as:

$$h_{CH46} := 600.00 \cdot \frac{\text{kJ}}{\text{kg}}$$

Methane enthalpy at 297.0 psia and 160 K was calculated using Refprops and is given as:

$$h_{CH47} := 184.53 \cdot \frac{\text{kJ}}{\text{kg}}$$

Methane enthalpy at 296.5 psia and 140 K was calculated using Refprops and is given as:

$$h_{CH48} := 104.41 \cdot \frac{\text{kJ}}{\text{kg}}$$

Methane enthalpy at 296.0 psia and 120 K was calculated using Refprops and is given as:

$$h_{CH49} := 31.90 \cdot \frac{\text{kJ}}{\text{kg}}$$

The enthalpy, density, and entropy for Methane after isenthalpic expansion of subcooled LNG at ~296 psia and 120 K to the Bubble Point temperature at 30 psia and 120.7 K were calculated using Refprops and are given as:

$$h_{CH4Liq} := 31.90 \cdot \frac{\text{kJ}}{\text{kg}}$$

$$\rho_{CH41207Liq} := 408.84 \cdot \frac{\text{kg}}{\text{m}^3}$$

$$s_{CH41207liq} := 0.2725 \cdot \frac{\text{kJ}}{\text{kg} \cdot \text{K}}$$

The ideal work rate for liquefaction of methane (i.e., PNG) can now be calculated for the feed gas conditions and LNG final conditions that are restated here.

$$T_{H1} := 280 \cdot \text{K}$$

$$T_{CLig} 120.7 \cdot \text{K}$$

$$\text{volrate}_{CH4} := 1000 \cdot \text{gpd}$$

The LNG production rate is a design variable that can be selected; the mass flow rate is calculated from the volume flow rate by multiplying by the liquid natural gas (LNG) density:

$$massrate_{CH4} := volrate_{CH4} \cdot \rho_{CH41207Liq}$$

$$massrate_{CH4} = 0.018\ \frac{\text{kg}}{\text{s}}$$

$$s_{CH4280} = 4.916 \cdot \frac{\text{kJ}}{\text{kg} \cdot \text{K}}$$

$$h_{CH41} = 847.88 \cdot \frac{\text{kJ}}{\text{kg}}$$

Coming from Refprops

$$s_{CH41207liq} = 0.273 \cdot \frac{\text{kJ}}{\text{kg} \cdot \text{K}}$$

$$h_{CH4Liq} = 31.9 \cdot \frac{\text{kJ}}{\text{kg}}$$

$$W_{dotLNGideal} := \text{massrate}_{CH4}[T_{H1} \cdot (s_{CH4280} - s_{CH41207liq}) + (h_{CH4Liq} - h_{CH41})]$$

$$W_{dotLNGideal} = 8.674 \times 10^3\ \text{W}$$

Note: the higher PNG pressure and pre-cooling to 280 K substantially reduce specific liquefaction energy for LNG (by ~50% from the value in Barron's book of ~1050 kJ/kg))!!

$$W_{spLNGideal} := \frac{W_{dotLNGideal}}{massrate_{CH4}}$$

$$W_{spLNGideal} = 484.228 \cdot \frac{\text{kJ}}{\text{kg}}$$

Now calculate process stream cooling, liquefaction, and subcooling thermal loads for each stage of the AMRL for a 300 psia pipeline natural gas (PNG) process stream (that is predominately methane as assumed here).

$$Q_{dotCH4260K} := \text{massrate}_{CH4} \cdot (h_{CH42} - h_{CH41})$$

$$Q_{dotCH4260K} = -838.298\ \text{W}$$

$$Q_{dotCH4240K} := \text{massrate}_{CH4}'(h_{CH43} - h_{CH42})$$

$$Q_{dotCH4240K} = -844.03\ \text{W}$$

$$Q_{dotCH4220K} := \text{massrate}_{CH4} \cdot (h_{CH44} - h_{CH43})$$

$$Q_{dotCH4220K} == -862.122\ \text{W}$$

$$Q_{dotCH4200K} := \text{massrate}_{CH4} \cdot (h_{CH45} - h_{CH44})$$

$$Q_{dotCH4200K} = -902.246\ \text{W}$$

$$Q_{dotCH4180K} := \text{massrate}_{CH4} \cdot (h_{CH46} - h_{CH45})$$

$$Q_{dotCH4180K} = -993.419\ \text{W}$$

The latent heat of liquefaction is large as exhibited in the larger enthalpy below:

$$Q_{dotCH4160K} := \text{massrate}_{CH4} \cdot (h_{CH47} - h_{CH46})$$

$$Q_{dotCH4160K} = -7.442 \times 10^3\ \text{W}$$

$$Q_{dotCH4140K} := \text{massrate}_{CH4} \cdot (h_{CH48} - h_{CH47})$$

$$Q_{dotCH4140K} = -1{,}435 \times 10^3\ \text{W}$$

$$Q_{dotCH4120K} := \text{massrate}_{CH4} \cdot (h_{CH49} \cdot h_{CH48})$$

$$Q_{dotCH4120K} = -1.299 \times 10^3\ \text{W}$$

[0070] The sum of these thermal loads gives the total process cooling load as:

$$Q_{dotCH4load} = -1.462 \times 10^4\ \text{W}$$

The negative sign comes from choice of the control volume (CV); i.e. heat leaving the process stream control volume is taken as negative by convention.

[0071] Use an 8-stage AMRR with NG entering at 280 K into 8 counterflow HEXs each cooled by cold He gas from each 20-K stage of the refrigerator. As a baseline assume no bypass flow so the NG process thermal load at each stage must be pumped from the average Tcold to the average Thot for that stage. The reject heat from a colder stage is part of the thermal load for the next warmer stage. A small parasitic heat leak is added at each stage. Each AMRR stage has two sets of dual-regenerators with simulated high efficiency for a good design; this real effect is also an additional input parameter. NOW calculate total thermal loads for PNG for ascending stages for SERIES liquefier configuration, i.e., the thermal load from bottom or next lower stage and the work input for the bottom or next lower stage become an additional thermal load for each stage and similarly up to the 1st stage. Also consider estimated irreversible entropy in each stage by using a relative efficiency of each stage (η_{stage}) when calculating rate of work to lift the thermal loads from lower T to higher T. NO pre-cooling of NG from the bypass flow is assumed so process thermal load at Tcold is added to colder stage thermal load on each AMRR stage. A small parasitic heat leak is also added at each stage for completeness.

$$\eta_{stage} := 0.85$$

$$Q_{dotparasitic} := 2 \cdot W$$

The average hot and cold temperatures of the eight stage (coldest one) are given as:

$$T_{H8} := 140 \cdot \text{K}$$

$$T_{C8} := 120 \cdot \text{K}$$

The rate of work for the eight stage with its thermal loads is calculated as follows:

$$W_{dotCH48} := \frac{(-Q_{dotCH4120K} + Q_{dotparasitic})}{\eta_{stage}} \cdot \left(\frac{T_{H8}}{T_{C8}} - 1\right)$$

$$W_{dotCH48} = 255.064\ \text{W}$$

$$Q_{dotCH4H8} := (-Q_{dotCH4120K} + Q_{dotparasitic}) + W_{dotCH48}$$

$$Q_{dotCH4H8} = 1.556 \times 10^3\ \text{W}$$

The rate of work for the seventh stage with its thermal loads is calculated as follows:

$$T_{H7} := 160 \cdot \text{K}$$

$$T_{C7} := 140 \cdot \text{K}$$

-continued

$$W_{dotCH47} := \frac{[(-Q_{dotCH4140K} + Q_{dotparasitic}) + Q_{dotCH4H8}]}{\eta_{stage}} \cdot \left(\frac{T_{H7}}{T_{C7}} - 1\right)$$

$$W_{dotCH47} = 503.03 \text{ W}$$

$$Q_{dotCH4H7} := (-Q_{dotCH4140K} + Q_{dotparasitic} + Q_{dotCH4H8}) + W_{dotCH47}$$

$$Q_{dotCH4H7} = 3.496 \times 10^3 \text{ W}$$

A similar set of calculations is done for each stage as shown below:

$$T_{H6} := 180 \cdot \text{K}$$

$$T_{C6} := 160 \cdot \text{K}$$

$$W_{dotCH46} := \frac{[(-Q_{dotCH4160K} + Q_{dotparasitic}) + Q_{dotCH4H7}]}{\eta_{stage}} \cdot \left(\frac{T_{H6}}{T_{C6}} - 1\right)$$

$$W_{dotCH46} = 1.609 \times 10^3 \text{ W}$$

$$Q_{dotCH4H6} := (-Q_{dotCH4160K} + Q_{dotparasitic} + Q_{dotCH4H7}) + W_{dotCH46}$$

$$Q_{dotCH4H6} = 1.255 \times 10^4 \text{ W}$$

$$T_{H5} := 200 \cdot \text{K}$$

$$T_{C5} := 180 \cdot \text{K}$$

$$W_{dotCH45} := \frac{[(-Q_{dotCH4180K} + Q_{dotparasitic}) + Q_{dotCH4H6}]}{\eta_{stage}} \cdot \left(\frac{T_{H5}}{T_{C5}} - 1\right)$$

$$W_{dotCH45} = 1.771 \times 10^3 \text{ W}$$

$$Q_{dotCH4H5} := (-Q_{dotCH4180K} + Q_{dotparasitic} + Q_{dotCH4H6}) + W_{dotCH45}$$

$$Q_{dotCH4H5} = 1.531 \times 10^4 \text{ W}$$

$$T_{H4} := 220 \cdot \text{K}$$

$$T_{C4} := 200 \cdot \text{K}$$

$$W_{dotCH44} := \frac{[(-Q_{dotCH4200K} + Q_{dotparasitic}) + Q_{dotCH4H5}]}{\eta_{stage}} \cdot \left(\frac{T_{H4}}{T_{C4}} - 1\right)$$

$$W_{dotCH44} = 1.908 \times 10^3 \text{ W}$$

$$Q_{dotCH4H4} := (-Q_{dotCH4200K} + Q_{dotparasitic} + Q_{dotCH4H5}) + W_{dotCH44}$$

$$Q_{dotCH4H4} = 1.813 \times 10^4 \text{ W}$$

$$T_{H3} := 240 \cdot \text{K}$$

$$T_{C3} := 220 \cdot \text{K}$$

$$W_{dotCH43} := \frac{[(-Q_{dotCH4220K} + Q_{dotparasitic}) + Q_{dotCH4H4}]}{\eta_{stage}} \cdot \left(\frac{T_{H3}}{T_{C3}} - 1\right)$$

$$W_{dotCH43} = 2.031 \times 10^3 \text{ W}$$

$$Q_{dotCH4H3} := (-Q_{dotCH4220K} + Q_{dotparasitic} + Q_{dotCH4H4}) + W_{dotCH43}$$

$$Q_{dotCH4H3} = 2.102 \times 10^4 \text{ W}$$

$$T_{H2} := 260 \cdot \text{K}$$

$$T_{C2} := 240 \cdot \text{K}$$

$$W_{dotCH42} := \frac{[(-Q_{dotCH4240K} + Q_{dotparasitic}) + Q_{dotCH4H3}]}{\eta_{stage}} \cdot \left(\frac{T_{H2}}{T_{C2}} - 1\right)$$

$$W_{dotCH42} = 2.144 \times 10^3 \text{ W}$$

$$Q_{dotCH4H2} := (-Q_{dotCH4240K} + Q_{dotparasitic} + Q_{dotCH4H3}) + W_{dotCH42}$$

$$Q_{dotCH4H2} = 2.401 \times 10^4 \text{ W}$$

$$T_{H1} := 280 \cdot \text{K}$$

-continued

$$T_{C1} := 260 \cdot \text{K}$$

$$W_{dotCH41} := \frac{[(-Q_{dotCH4260K} + Q_{dotparasitic}) + Q_{dotCH4H2}]}{\eta_{stage}} \cdot \left(\frac{T_{H1}}{T_{C1}} - 1\right)$$

$$W_{dotCH41} = 2.249 \times 10^3 \text{ W}$$

$$Q_{dotCH4H1} := (-Q_{dotCH4260K} + Q_{dotparasitic} + Q_{dotCH4H2}) + W_{dotCH41}$$

$$Q_{dotCH4H1} = 2.71 \times 10^4 \text{ W}$$

$$W_{dotTOTALnobp} := W_{dotCH48} + W_{dotCH47} + W_{dotCH46} + W_{dotCH45} + W_{dotCH44} + W_{dotCH43} + W_{dotCH42} + W_{dotCH41}$$

$$W_{dotTOTALnobp} = 1.247 \times 10^4 \text{ W}$$

$$FOM := \frac{W_{dotLNGideal}}{W_{dotTOTALnobp}}$$

$$FOM = 0.696$$

In this case there is a small parasitic load but no HTF pump power

Stage No. and Temperature Span (K)	NG Process Stream Thermal Load (kW)	Total Reject Heat Load per Stage (kW)	Work Rate for Each Stage (kW)
1: 280 to 260	0.841	257.8	22.4
2: 260 to 240	0.848	227.0	21.0
3: 240 to 220	0.866	197.4	19.5
4: 220 to 200	0.907	169.2	18.0
5: 200 to 180	1.020	142.1	16.2
6: 180 to 160	7.452	115.9	10.6
7: 160 to 140	1.439	30.68	3.36
8: 140 to 120	1.175	12.88	1.08

Table of Temperature ranges, CH4 process stream loads, total heat reject loads, and work rates for each stage for 10,000 gal/day of LNG. These are 10 times larger than for 1,000 gal/day of LNG and also include irreversible entropy.

[0072] The calculation of the various mechanisms that affect the FOM was done for the 8-stage AMRL for LNG to show their relative magnitudes and where to focus the design efforts for higher FOM. Contributions to FOM by mechanism are summarized in the table below.

10,000 Gal/Day LNG F.O.M. Calculation	Work rate (kW)
Carnot work for 8 stage system (cool from 280 K to 120 K @ 35 psia)*	83.2
Internal irreversible entropy sources	28.9
Parasitic heat leak	0.4
Drives for regenerators	11.2
HTF pumps	1.1
Cryocooler compressor	8
Total real work	132.9
Total ideal work	87.2
$FOM = \frac{\dot{W}_{Ideal}}{\dot{W}_{Real}}$	0.66

*Without by-pass flow this increases to 99 kW decreases to 0.57

[0073] FIG. **4** is a three-dimensional representation of the liquefier components houses within the cold box. The cryo-coolers **72**, elliptical magnets **76**, Rotary AMR devices **78**, drive mechanisms **80** (for moving the magnetic regenerators

in and out of the field), HTF circulation pumps **84**, cryopump **82** and magnetic flux return materials **74** will all be in the cold box. The arrangement of the ten magnets **76** and eight AMR devices **78** are shown with the AMR devices **78** sandwiched in between the magnets **76**. This configuration allows for a strong magnetic field for each AMR stage **78** which is generated by the combined fields of each magnet. The drives **80** and pumps **84** will be powered by mechanical forces created outside of the cold box, however each drive and pump will have their own transmissions to allow for unique drive and pump flow rates for each stage.

[0074] In the description provided herein, the term "about" means+/−20% of the indicated value or range unless otherwise indicated. The terms "a" and "an," as used herein, refer to one or more of the enumerated components or items. The use of alternative language (e.g., "or") will be understood to mean either one, both or any combination of the alternatives, unless otherwise expressly indicated. The terms "include" and "comprise" and "have" are used interchangeably and each of these terms, and variants thereof, are intended to be construed as being non-limiting. In view of the many possible embodiments to which the principles of the disclosed invention may be applied, it should be recognized that the illustrated embodiments are only preferred examples of the invention and should not be taken as limiting the scope of the invention.

[0075] It will be appreciated that the methods and systems of the present invention may be embodied in a variety of different forms, and that the specific embodiments shown in the figures and described herein are presented with the understanding that the present disclosure is considered exemplary of the principles of the invention and is not intended to limit any claimed subject matter to the illustrations and description provided herein. The various embodiments described may be combined to provide further embodiments. The described devices, systems, methods and compositions may omit some elements or steps, add other elements or steps, or combine the elements or execute steps in a different combination or order than that specifically described.

We claim:

1. A process for liquefying process gases comprising:

introducing a high-pressure helium or liquid propane heat transfer fluid into each stage of a multi-stage active magnetic regenerative refrigerator apparatus, wherein each active magnetic regenerative refrigerator stage comprises: (i) a high magnetic field portion in which the heat transfer fluid flows from a cold side to a hot side through at least one magnetized regenerator having at least one magnetic refrigerant, (ii) a first no heat transfer fluid flow portion in which the regenerator is demagnetized, (iii) a low magnetic field portion in which the heat transfer fluid flows from a hot side to a cold side through at least one demagnetized regenerator, and (iv) a second no heat transfer fluid flow portion in which the regenerator is magnetized;

within each stage of the multi-stage active magnetic regenerative refrigerator apparatus, continuously introducing a separate flow of the heat transfer fluid from the cold side of the low magnetic field portion into the cold side of the high magnetic field portion; and

continuously separating a portion of the cold heat transfer fluid flowing from the cold side of the low magnetic field portion of each stage to generate an unbalanced flow stream from each stage, returning the separated cold heat transfer fluid at each stage through a process gas heat exchanger to cool the process gas before the heat transfer fluid rejoins the primary heat transfer stream near the hot temperature of each stage near the inlet to a fluid circulating means.

2. The process of claim **1**, wherein each active magnetic regenerative refrigerator stage comprises a different magnetic refrigerant material having a different Curie temperature and each magnetic refrigerant material comprises at least one of the following materials: Gd, $Gd_{0.90}Y_{0.10}$, $Gd_{0.83}Dy_{0.17}$, $Gd_{0.30}Tb_{0.70}$, $Gd_{0.69}Er_{0.31}$, $Gd_{0.02}Tb_{0.98}$, $Gd_{0.32}Dy_{0.68}$, $Gd_{0.66}Y_{0.34}$, $Gd_{0.39}Ho_{0.61}$, $Gd_{0.59}Y_{0.41}$, $Gd_{0.15}Dy_{0.85}$, $Gd_{0.42}Er_{0.58}$, $Gd_{0.27}Ho_{0.73}$, $Gd_{0.16}Ho_{0.84}$, $Gd_{0.34}Er_{0.66}$, $Gd_{0.23}Er_{0.77}$.

3. A process for liquefying a process gas comprising:

introducing a heat transfer fluid into an active magnetic regenerative refrigerator apparatus that comprises from about 4 to about 13 successive stages, wherein each stage comprises an independently compositionally distinct magnetic refrigerant material having an independent Curie temperature, and wherein the first stage has the highest Curie temperature and the last stage has the lowest Curie temperature.

4. The process of claim **3**, additionally comprising:

flowing different rates of heat transfer fluid through each stage of the active magnetic regenerative refrigerator apparatus to cool each stage during start up until the magnetic refrigerants in each stage are cooled below their respective Curie temperatures.

5. The process of claim **3**, additionally comprising:

flowing bypass heat transfer fluid flow from each stage through a process heat exchanger and removing sensible heat from the process stream in each stage; and cooling the bypass fluid flow by the same temperature as an operating temperature range for each stage.

6. The process of claim **3**, additionally comprising:

flowing a primary heat transfer fluid from each stage through a thermal load heat exchanger and absorbing reject heat from the next lower stage and, in stages where the process stream liquefies, absorbing latent heat of liquefaction and parasitic heat leaks into the stage where liquefaction occurs.

7. The process of claim **5**, wherein the bypass flow comprises from about 3% to 12% of the heat transfer fluid flow.

8. The process of claim **5**, wherein the bypass flow comprises more than about 2% and less than about 20% of the heat transfer fluid flow.

9. The process of claim **5**, further comprising introducing a non-bypassed portion of the heat transfer fluid into the cold side of the magnetized bed in the high magnetic field section.

10. The process of claim **3**, wherein the overall process achieves a Figure of Merit (FOM) of at least 0.6.

11. The process of claim **3**, wherein each distinct magnetic regenerative refrigerator material comprises at least one of the following materials: Gd, $Gd_{0.90}Y_{0.10}$, $Gd_{0.83}Dy_{0.17}$, $Gd_{0.30}Tb_{0.70}$, $Gd_{0.69}Er_{0.31}$, $Gd_{0.02}Tb_{0.98}$, $Gd_{0.32}Dy_{0.68}$, $Gd_{0.66}Y_{0.34}$, $Gd_{0.39}Ho_{0.81}$, $Gd_{0.59}Y_{0.41}$, $Gd_{0.15}Dy_{0.85}$, $Gd_{0.42}Er_{0.58}$, $Gd_{0.27}Ho_{0.73}$, $Gd_{0.16}Ho_{0.84}$, $Gd_{0.34}Er_{0.66}$, $Gd_{0.23}Er_{0.77}$.

12. An active magnetic regenerative liquefier comprising:

multiple successive active magnetic regenerator stages, wherein each stage comprises an independently com-

positionally distinct magnetic refrigerant material having an independent Curie temperature, and wherein the first stage has the highest Curie temperature and the last stage has the lowest Curie temperature.

13. The active magnetic regenerative liquefier of claim **12**, wherein each successive stage has a Curie temperature from about 20 to about 40K different from the neighboring stages, and the stages are arranged in successive Curie temperature order with a first stage having the highest Curie temperature and highest magnetic refrigerant material mass and a final stage having the lowest Curie temperature and lowest magnetic refrigerant material mass.

14. The active magnetic regenerative liquefier of claim **12**, wherein each magnetic refrigerant is constrained to operate near and below its Curie temperature throughout an active magnetic regeneration cycle.

15. The active magnetic regenerative liquefier of claim **12**, wherein temperature ranges across the highest to lowest Curie temperature stages range from about 285 K to about 120 K.

16. The active magnetic regenerative liquefier of claim **12**, wherein each stage comprises a unique magnetocaloric alloy.

17. The active magnetic regenerative liquefier of claim **12**, wherein each distinct magnetic refrigerator material comprises at least one of the following materials: Gd, $Gd_{0.90}Y_{0.10}$, $Gd_{0.83}Dy_{0.17}$, $Gd_{0.30}Tb_{0.70}$, $Gd_{0.69}Er_{0.31}$, $Gd_{0.02}Tb_{0.98}$, $Gd_{0.32}Dy_{0.68}$, $Gd_{0.66}Y_{0.34}$, $Gd_{0.39}Ho_{0.61}$, $Gd_{0.59}Y_{0.41}$, $Gd_{0.15}Dy_{0.85}$, $Gd_{0.42}Er_{0.58}$, $Gd_{0.27}Ho_{0.73}$, $Gd_{0.16}Ho_{0.84}$, $Gd_{0.34}Er_{0.66}$, $Gd_{0.23}Er_{0.77}$.

18. The active magnetic regenerative liquefier of claim **12**, comprising eight stages, each stage having a different magnetocaloric alloy refrigerant material.

* * * * *